Turkish Journal of Mathematics

Volume 47 | Number 2 Article 9

1-1-2023

Numerical solution for Benjamin-Bona-Mahony-Burgers equation with Strang time-splitting technique

MELİKE KARTA

Turkish Journal of Mathematics

http://journals.tubitak.gov.tr/math/

Research Article

Turk J Math
(2023) 47: 537 – 553
© TÜBİTAK
doi:10.55730/1300-0098.3377

Numerical solution for Benjamin-Bona-Mahony-Burgers equation with Strang time-splitting technique

Melike KARTA*
Department of Mathematics, Faculty of Science and Arts, Ağrı İbrahim Çeçen University, Ağrı, Turkey

Received: 15.08.2022 • **Accepted/Published Online:** 04.01.2023 • **Final Version:** 09.03.2023

Abstract: In the present manuscript, the Benjamin-Bona-Mahony-Burgers (BBMB) equation will be handled numerically by Strang time-splitting technique. While applying this technique, collocation method based on quintic B-spline basis functions is applied. In line with our purpose, after splitting the BBM-Burgers equation given with appropriate initial boundary conditions into two subequations containing the derivative in terms of time, the quintic B-spline based collocation finite element method (FEM) for spatial discretization and the suitable finite difference approaches for time discretization is applied to each subequation and hereby two different systems of algebraic equations are obtained. Four test problems are utilized to test the efficiency and reliability of the presented method. The error norms L_2 and L_∞ with mass, energy, and momentum conservation constants I_1, I_2 and I_3, respectively, are computed. To do a comparison with the other studies in the literature, the newly found approximate solutions are exhibited in both tabular and graphical formats. Also, stability analysis of numerical approach by the von Neumann method is researched.

Key words: BBMB equation, quintic B-splines, collocation method, Strang splitting

1. Introduction

Bruzon and Gandarias [7] considered a generalized BBM-Burgers equation given as

$$U_t - U_{xxt} - \alpha U_{xx} + \beta U_x + (g(U))_x = 0, \tag{1.1}$$

in which α is a given nonnegative real-number, $\beta \in R$ and $g(U)$ is a predefined nonlinear function. Peregrine [43] first proposed equation and Benjamin et al. [5] broadly explained it. In this article, by taking $g(U) = \frac{U^2}{2}$, we are going to handle the BBM-Burgers equation as follows:

$$U_t - U_{xxt} - \alpha U_{xx} + \beta U_x + UU_x = 0, \quad x \in [x_L, x_R], t \in [0, T], \tag{1.2}$$

with the condition given at initial time

$$U(x, 0) = g_0(x), \tag{1.3}$$

and the conditions given at the boundaries

$$\begin{aligned} U(x_L, t) &= U(x_R, t) = 0, \\ U_x(x_L, t) &= U_x(x_R, t) = 0, \\ U_{xx}(x_L, t) &= U_{xx}(x_R, t) = 0 \quad t > 0. \end{aligned} \tag{1.4}$$

*Correspondence: mkarta@agri.edu.tr
2010 *AMS Mathematics Subject Classification:* 65D07, 65L60

If $\alpha = 0$ is taken in Eq. (1.2), the (RLW) equation is obtained in form

$$U_t - U_{xxt} + \beta U_x + UU_x = 0 \tag{1.5}$$

and this is named as the Benjamin-Bona-Mahony (BBM) equation. The approximate solution of the BBM-Burgers equation is the subject of research by many authors using various methods. Among them, Jain et al. [30] solved BBM equation with a combination of the splitting method and cubic B-spline technique. Gardner et al. [22] applied A B-spline finite element method (FEM) involving Galerkin method based on quadratic B-splines. Gardner et al. [23] presented a least-squares techniques, Doğan [16] investigated equation using Galerkin method via linear space finite elements. Soliman and Raslan [46] and Soliman and Hussien [47] proposed quadratic and septic splines collocation method, respectively. Dağ et al. [17] studied with cubic B-spline collocation finite element method. Esen and Kutluay [20] used quadratic B-spline lumped Galerkin method and in the same year they [32] presented a linearized finite difference method for equation. Omrani and Ayadi [41] used finite difference method and also showed with the Brower's fixed point theorem to existence of solutions. Moreover, Arora et al. [1] utilized collocation method with quartic B-spline for the BBMB equation. Yağmurlu et al. [53] solved by the Strang splitting technique using the finite element collocation method with cubic B-splines. Karakoç and Bhowmik [31] implemented a lumped Galerkin technique to the BBM-Burgers equation and founded to the existence and uniqueness of solutions. Zarebnia and Parvaz [54–57] proposed collocation method based on cubic, quadratic and quintic B-splines for the numerical algorithm of BBM-Burgers equation, respectively. Also, related studies for approximate solutions of the equation can be found as [3, 4, 6, 9, 21, 40, 45], [34–37] and [10–15]. Mehdi et al. [18] performed a finite difference formula for solving numerically of the generalized BBM-Burgers equation and then applied the energy method for the stability and convergence analyses. Zhang et al. [58] suggested two linearized finite difference schemes and proved convergence and unique solvability of the BBMB equation with the convergence order $O(\tau^2 + h^2)$. Arora et al. [2] improved a hybrid technique including quintic Hermite splines collocation method (QHCM) for solving numerically of the BBM-Burgers equation. For studies on the splitting technique, the reader may refer to [24–29] and [33, 39, 42, 48, 50, 52, 59].

We can say that the problem discussed throughout the article can be solved more effectively and faster numerically by Strang time-splitting technique combined with quintic B-spline collocation method. This article is designed as follows: In Section 2, a brief information about the Strang time-splitting technique is given. In Section 3 after explaining the collocation method with quintic B-spline in detail, Eq. (1.2) is split into two subequations and each of them is solved numerically with Strang time-splitting technique by applying the quintic B-spline collocation method. Also, In Section 4, the stability analysis for the numerical approach otained with the present method is examined. In Section 5, four test problems are offered, one of which is inhomogeneous BBM-Burgers equation and the others are BBM-Burgers equations given by different initial condition and in this section the error norms L_2 and L_∞ with invariant values I_1, I_2 and I_3 are calculated to analyze the effectiveness and accuracy of the presented method and the computed values are given in tables and graphics to compare with existing studies in the literature. Lastly, Section 6 presents a brief conclusion as an overview.

2. Strang time-splitting technique

Before proceeding to the application of the method, it would be appropriate to give information about the Strang splitting technique, which is of great importance in the approximate solution for the given problem. To use this technique, the given complex problem is first divided into simpler two subproblems with smaller time steps. If a Cauchy problem is assumed to have the following form

$$\frac{dU(t)}{dt} = \hat{A}U(t) + \hat{B}U(t), \quad U(0) = U_0, \quad t \in [0, T]. \tag{2.1}$$

Then, the problem is split into such that $\frac{dU}{dt} = \hat{A}U$, $\frac{dU}{dt} = \hat{B}U$ where $U(x,t)$ is a semidiscretized function given on spatial direction and $\hat{A}$ and $\hat{B}$ are lie operators. In this case, the proposed technique tries to solve Eq. (1.2) either numerically or analitically [8]. Let the exact or numerical solutions of the equations containing the operators $\hat{A}$ and $\hat{B}$ in $\frac{dU}{dt} = \hat{A}U$, $\frac{dU}{dt} = \hat{B}U$ be $\rho_{\Delta t}^{[\hat{A}]}$ and $\rho_{\Delta t}^{\hat{B}}$, and let $\psi_{\Delta t}$ be the exact solution of the equation (2.1). In this case, first-order splitting methods are defined as [51]

$$\rho_{\Delta t}^{[\hat{B}]} o \rho_{\Delta t}^{[\hat{A}]} = e^{\Delta t \hat{B}} e^{\Delta t \hat{A}} \text{ or } \rho_{\Delta t}^{[\hat{A}]} o \rho_{\Delta t}^{[\hat{B}]} = e^{\Delta t \hat{A}} e^{\Delta t \hat{B}}.$$

With the aid of the Taylor series, for an initial value U_0 it is seen that there is a first-order approximation to the solution of equation (2.1) as follows:

$$\psi_{\Delta t}(U_0) = (\rho_{\Delta t}^{[\hat{A}]} o \rho_{\Delta t}^{[\hat{B}]})(U_0) + 0(\Delta t^2).$$

Exchanging the operators $\hat{A}$ and $\hat{B}$, combination for half time steps can be taken as follows:

$$U(t_{n+1}) = (e^{\frac{\Delta t}{2}\hat{A}} e^{\frac{\Delta t}{2}\hat{B}})(e^{\frac{\Delta t}{2}\hat{B}} e^{\frac{\Delta t}{2}\hat{A}})U(t_n)$$

$$= e^{\frac{\Delta t}{2}\hat{A}} e^{\Delta t \hat{B}} e^{\frac{\Delta t}{2}\hat{A}} U(t_n).$$

Then we can characterize the approach mentioned as

$$S_{\Delta t} = e^{\frac{\Delta t}{2}\hat{A}} e^{\Delta t \hat{B}} e^{\frac{\Delta t}{2}\hat{A}} \text{ or } S_{\Delta t}^{*} = e^{\frac{\Delta t}{2}\hat{B}} e^{\Delta t \hat{A}} e^{\frac{\Delta t}{2}\hat{B}}.$$

As it is widely known, this is referred to as Strang splitting technique [38] which have the "$\hat{A} - \hat{B} - \hat{A}$" and "$\hat{B} - \hat{A} - \hat{B}$" or the so-called symmetric Marchuk. The procedure for Strang splitting scheme can be presented as

$$\begin{aligned}
\frac{dU^{*}(t)}{dt} &= \hat{A}U^{*}(t), \quad U^{*}(0) = U_0, && t \in \left[t_n, t_{n+\frac{1}{2}}\right] \\
\frac{dU^{**}(t)}{dt} &= \hat{B}U^{**}(t), \quad U^{**}(0) = U^{*}(\frac{\Delta t}{2}), && t \in [t_n, t_{n+1}] \\
\frac{dU^{***}(t)}{dt} &= \hat{A}U^{***}(t), \quad U^{***}(0) = U^{**}(\Delta t), && t \in \left[t_n, t_{n+\frac{1}{2}}\right].
\end{aligned} \tag{2.2}$$

in which $t_{n+1} = t_n + \Delta t$, $t_{n+\frac{1}{2}} = t_n + \frac{\Delta t}{2}$. Here the desired solutions are easily obtained through the equation of $U(t_{n+1}) = U^{***}(t_{n+1})$. The formal solution of Equation (2.1) is written as $U(t_{n+1}) = e^{\Delta t(\hat{A}+\hat{B})}U(t_n)$, where $\Delta t = t_{n+1} - t_n$ is the time step. Taylor series expansion of this solution can be expressed as

$$U(t_{n+1}) = e^{\Delta t(\hat{A}+\hat{B})}U(t_n) = \sum_{k=0}^{\infty} \frac{t^k}{k!} \big(\hat{A}(u(t))\frac{\partial}{\partial U} + \hat{B}(u(t))\frac{\partial}{\partial U}\big)^k U(t_n).$$

It is obtained in the following form such that T_e is a local truncation error

$$U(t_{n+1}) = e^{\Delta t(\hat{A}+\hat{B})}U(t_n) \approx e^{\frac{\Delta t}{2}\hat{A}}e^{\Delta t\hat{B}}e^{\frac{\Delta t}{2}\hat{A}} + \Delta t T_e$$

$$T_e = \frac{1}{\Delta t}\Big[e^{\Delta t(\hat{A}+\hat{B})} - e^{\frac{\Delta t}{2}\hat{A}}e^{\Delta t\hat{B}}e^{\frac{\Delta t}{2}\hat{A}}\Big]U(t_n). \tag{2.3}$$

If the Taylor series expansion of the $e^{\Delta t(\hat{A}+\hat{B})}$ and $e^{\frac{\Delta t}{2}\hat{A}}e^{\Delta t\hat{B}}e^{\frac{\Delta t}{2}\hat{A}}$ exponential functions are substituted in (2.3), the local truncation error T_e called as splitting error is obtained as follows:

$$T_e = \frac{\Delta t^2}{24}\Big(\Big[\hat{A},\Big[\hat{B},\hat{A}\Big]\Big] - \Big[\hat{B},\Big[\hat{A},\hat{B}\Big]\Big]\Big)U(t_n) + O(\Delta t^3)$$

and this shows the fact that the proposed technique is of the second-order.

3. Collocation method via quintic B-spline

Before starting the numerical process, initially the interval $x_L \le x \le x_R$ is partitioned into uniformly such that $h = x_m - x_{m+1} = \frac{x_R - x_L}{N}$ by knots x_m in which $(m = 0(1)N-1)$ and $x_L = x_0 < x_1 < ... < x_N = x_R$. The quintic B-spline functions $\varphi_m(x)$ on $[x_L, x_R]$ stated as the solution region for $(m = -2(1)N+2)$ at the nodes x_m are introduced as follows [44]:

$$\varphi_m(x) = \frac{1}{h^5}\begin{cases} (x-x_{m-3})^5, & x\in[x_{m-3},x_{m-2}] \\ (x-x_{m-3})^5 - 6(x-x_{m-2})^5, & x\in[x_{m-2},x_{m-1}] \\ (x-x_{m-3})^5 - 6(x-x_{m-2})^5 + 15(x-x_{m-1})^5, & x\in[x_{m-1},x_m] \\ (x_{m+3}-x)^5 - 6(x_{m+2}-x)^5 + 15(x_{m+1}-x)^5, & x\in[x_m,x_{m+1}] \\ (x_{m+3}-x)^5 - 6(x_{m+2}-x)^5, & x\in[x_{m+1},x_{m+2}] \\ (x_{m+3}-x)^5, & x\in[x_{m+2},x_{m+3}] \\ 0, & otherwise. \end{cases} \tag{3.1}$$

For detailed information, the reader can refer to Ref. [19] related to B-slines. All of the quintic basis functions are zero on the element $[x_m, x_m+1]$ except those $\varphi_{m-2}(x), \varphi_{m-1}(x), \varphi_m(x), \varphi_{m+1}(x), \varphi_{m+2}(x),\ \varphi_{m+3}(x)$. The approximate solution $U_N(x,t)$ of Eq. (1.2) on $[x_m, x_{m+1}]$ can be described as

$$U_N^e(x,t) = \sum_{j=m-2}^{m+3}\varphi_j(x)\delta_j(t)\ , \tag{3.2}$$

where $\varphi_j(x)$ $(j = (m-2)(1)(m+3))$ are B-spline element functions and $\delta_j(t)$ $(j = m-2, m-1, ..., m+3)$ are time-dependent element parameters to be found out. The values of U_N^e and its first and second order derivatives with respect to variable x at the nodal points x_m can be calculated in terms of δ_m

$$\begin{aligned} U_N^e(x_m,t) = (U_N^e)_m &= (\delta_{m-2} + 26\delta_{m-1} + 66\delta_m + 26\delta_{m+1} + \delta_{m+2}) \\ (U_N^e)'_m = U'_m &= \frac{5}{h}(-\delta_{m-2} - 10\delta_{m-1} + 10\delta_{m+1} + \delta_{m+2}) \\ (U_N^e)''_m = U''_m &= \frac{20}{h^2}(\delta_{m-2} + 2\delta_{m-1} - 6\delta_m + 2\delta_{m+1} + \delta_{m+2}). \end{aligned} \tag{3.3}$$

Eq. (1.2) can be split as follows:

$$U_t - U_{xxt} - \alpha U_{xx} + \beta U_x = 0 \tag{3.4}$$

$$U_t - U_{xxt} + UU_x = 0. \tag{3.5}$$

When the values of U and its first and second-order derivatives are used in Eqs. (3.4) and (3.5), one obtains the following system of algebraic equations

$$\begin{aligned} &\dot{\delta}_{m-2} + 26\dot{\delta}_{m-1} + 66\dot{\delta}_m + 26\dot{\delta}_{m+1} + \dot{\delta}_{m+2} - \frac{20}{h^2}(\dot{\delta}_{m-2} + 2\dot{\delta}_{m-1} - 6\dot{\delta}_m + 2\dot{\delta}_{m+1} + \dot{\delta}_{m+2}) \\ -&\frac{20\alpha}{h^2}(\delta_{m-2} + 2\delta_{m-1} - 6\delta_m + 2\delta_{m+1} + \delta_{m+2}) + \frac{5\beta}{h}(-\delta_{m-2} - 10\delta_{m-1} + 10\delta_{m+1} + \delta_{m+2}) = 0 \end{aligned} \tag{3.6}$$

$$\begin{aligned} &\dot{\delta}_{m-2} + 26\dot{\delta}_{m-1} + 66\dot{\delta}_m + 26\dot{\delta}_{m+1} + \dot{\delta}_{m+2} - \frac{20}{h^2}(\dot{\delta}_{m-2} + 2\dot{\delta}_{m-1} - 6\dot{\delta}_m + 2\dot{\delta}_{m+1} + \dot{\delta}_{m+2}) \\ &\qquad + \frac{5z_m}{h}(-\delta_{m-2} - 10\delta_{m-1} + 10\delta_{m+1} + \delta_{m+2}) = 0\ . \end{aligned} \tag{3.7}$$

Here, $''.''$ symbolizes the first derivative according to time t and z_m is considered

$$z_m = \delta_{m-2} + 26\delta_{m-1} + 66\delta_m + 26\delta_{m+1} + \delta_{m+2}$$

as a linearization scheme. The values $\delta_{-2}, \delta_{-1}, \delta_{N+1}$ and δ_{N+2} are found from U and its first derivative. In this case, we use z_m as an approximate value at the nodal points $(m = 0(1)N)$ until the until next time. That is;

$$\begin{aligned} z_0 &= 0, \\ z_1 &= \delta_{-1} + 26\delta_0 + 66\delta_1 + 26\delta_2 + \delta_3, \\ &\dots \\ z_{N-1} &= \delta_{N-3} + 26\delta_{N-2} + 66\delta_{N-1} + 26\delta_N + \delta_{N+1}, \\ z_N &= 0. \end{aligned} \tag{3.8}$$

By writing $\dfrac{\delta_m^{n+1} + \delta_m^n}{2}$ as Crank-Nicolson approximation instead of the parameter δ_m and $\dfrac{\delta_m^{n+1} - \delta_m^n}{\Delta t}$ as forward difference approximation instead of the parameter $\dot{\delta}_m$ in Eqs. (3.6) and (3.7), we can acquire a system of algebraic equations (3.9) and (3.10) given in the following

$$c_1\delta_{m-2}^{n+1} + c_2\delta_{m-1}^{n+1} + c_3\delta_m^{n+1} + c_4\delta_{m+1}^{n+1} + c_5\delta_{m+2}^{n+1} = c_6\delta_{m-2}^n + c_7\delta_{m-1}^n + c_8\delta_m^n + c_9\delta_{m+1}^n + c_{10}\delta_{m+2}^n \tag{3.9}$$

$$d_1\delta_{m-2}^{n+1} + d_2\delta_{m-1}^{n+1} + d_3\delta_m^{n+1} + d_4\delta_{m+1}^{n+1} + d_5\delta_{m+2}^{n+1} = d_6\delta_{m-2}^n + d_7\delta_{m-1}^n + d_8\delta_m^n + d_9\delta_{m+1}^n + d_{10}\delta_{m+2}^n \tag{3.10}$$

$$c_1 = 1 - \frac{20}{h^2} - \frac{10\alpha\Delta t}{h^2} - \frac{5\beta\Delta t}{2h}, c_2 = 26 - \frac{40}{h^2} - \frac{20\alpha\Delta t}{h^2} - \frac{25\beta\Delta t}{h}, c_3 = 66 + \frac{120}{h^2} + \frac{60\alpha\Delta t}{h^2}, c_4 = 26 - \frac{40}{h^2} - \frac{20\alpha\Delta t}{h^2} + \frac{25\beta\Delta t}{h},$$

$$c_5 = 1 - \frac{20}{h^2} - \frac{10\alpha\Delta t}{h^2} + \frac{5\beta\Delta t}{2h}, c_6 = 1 - \frac{20}{h^2} + \frac{10\alpha\Delta t}{h^2} + \frac{5\beta\Delta t}{2h}, c_7 = 26 - \frac{40}{h^2} + \frac{20\alpha\Delta t}{h^2} - \frac{25\beta\Delta t}{h}, c_8 = 66 + \frac{120}{h^2} - \frac{60\alpha\Delta t}{h^2},$$

$$c_9 = 26 - \frac{40}{h^2} + \frac{20\alpha\Delta t}{h^2} + \frac{25\beta\Delta t}{h}, c_{10} = 1 - \frac{20}{h^2} + \frac{10\alpha\Delta t}{h^2} - \frac{5\beta\Delta t}{2h}$$

$$d_1 = 1 - \frac{20}{h^2} - \frac{5z_m\Delta t}{2h}, d_2 = 26 - \frac{40}{h^2} - \frac{25z_m\Delta t}{h}, d_3 = 66 + \frac{120}{h^2}, d_4 = 26 - \frac{40}{h^2} + \frac{25z_m\Delta t}{h},$$

$$d_5 = 1 - \frac{20}{h^2} + \frac{5z_m\Delta t}{2h}, d_6 = 1 - \frac{20}{h^2} + \frac{5z_m\Delta t}{2h}, d_7 = 26 - \frac{40}{h^2} + \frac{25z_m\Delta t}{h}, d_8 = 66 + \frac{120}{h^2},$$

$$d_9 = 26 - \frac{40}{h^2} - \frac{25z_m\Delta t}{h}, d_{10} = 1 - \frac{20}{h^2} - \frac{5z_m\Delta t}{2h}.$$

The systems (3.9) and (3.10) include $(N+5)$ unknowns and $(N+1)$ equations. Since each system has dummy parameters δ_{-2}, δ_{-1} and $\delta_{N+1}, \delta_{N+2}$ which stand not inside the solution area, we first need to eliminate these illusory ones in order to obtain a unique solution of each system. For this reason, we have to use U and $U^{'}$ in Eq. (3.3) and the boundary conditions $U(x_L,t) = U(x_R,t) = 0$ and $U_x(x_L,t) = U_x(x_R,t) = 0$ in Eq. (1.4). Then we are able to obtain matrix system $(N+1)$ x $(N+1)$ for each of the above systems. The systems (3.9) and (3.10) are solved by Strang time-splitting technique and an inner iteration presented by form $(\delta^*)^n = \delta^n + \frac{1}{2}(\delta^n - \delta^{n-1})$ is applied 3 or 5 times throughout the computer run at every time step to the term of nonlinear z_m in Eq. (3.10) to acquire results closer to analytical solution.

The initial vector δ_m^0 is needed to solve systems (3.9) and (3.10). To calculate this initial vector, we can use the condition given at initial time

$$U(x,0) = g_0(x), \tag{3.11}$$

with the conditions given at the boundaries

$$\begin{aligned} U_x(x_L,t) &= U_x(x_L,t) = 0, \\ U_{xx}(x_L,t) &= U_{xx}(x_R,t) = 0. \end{aligned} \tag{3.12}$$

Therefore, to explain in more detail, this parameter is computed from the system of algebraic equations presented in the following form, found from the initial condition and its derivatives in Eq. (3)

$$\begin{aligned} \delta_{m-2}^0 + 26\delta_{m-1}^0 + 66\delta_m^0 + 26\delta_{m+1}^0 + \delta_{m+2}^0 &= g_0(x_m), m = 0(1)N \\ -\delta_{-2}^0 - 10\delta_{-1}^0 + 10\delta_1^0 + \delta_2^0 &= g_0^{'}(x_L) \\ \delta_{-2}^0 + 2\delta_{-1}^0 - 6\delta_0^0 + 2\delta_1^0 + \delta_2^0 &= g_0^{''}(x_L) \\ \delta_{N-2}^0 + 2\delta_{N-1}^0 - 6\delta_N^0 + 2\delta_{N+1}^0 + \delta_{N+2}^0 &= g_0^{''}(x_R) \\ -\delta_{N-2}^0 - 10\delta_{N-1}^0 + 10\delta_{N+1}^0 + \delta_{N+2}^0 &= g_0^{'}(x_R). \end{aligned} \tag{3.13}$$

Therefore, the matrix equation for the initial vector δ^0 is finally obtained as

$$\begin{bmatrix} 54 & 60 & 6 & & & & \\ 25.25 & 67.5 & 26.25 & 1 & & & \\ 1 & 26 & 66 & 26 & 1 & & \\ & & & \ddots & & & \\ & & 1 & 26 & 66 & 26 & 1 \\ & & & 1 & 26.25 & 67.5 & 25.25 \\ & & & & 6 & 60 & 54 \end{bmatrix} \begin{bmatrix} {\delta^0}_0 \\ {\delta^0}_1 \\ {\delta^0}_2 \\ . \\ . \\ . \\ {\delta^0}_{N-2} \\ {\delta^0}_{N-1} \\ {\delta^0}_N \end{bmatrix} = \begin{bmatrix} U_0 \\ U_1 \\ U_2 \\ . \\ . \\ . \\ U_{N-2} \\ U_{N-1} \\ U_N \end{bmatrix}.$$

4. Stability analysis

Here, we are going to investigate the stability analysis of numerical schemes (3.9) and (3.10) by von Neumann method [49]. Firstly, for the half-time step, writing the expressions $c_1, c_2, ..., c_9, c_{10}$ that we find in Section 3 and the expression $\delta_m^n = e^{i\gamma mh}\zeta^n$ in Eq. (3.9), we obtain equations in the following form after the necessary operations

$$\sigma_1 = \sigma_A\left(\frac{\zeta^{n+\frac{1}{2}}}{\zeta^n}\right) = \frac{A_1 + iB}{A_2 - iB}, \tag{4.1}$$

$$A_1 = (c_1 + c_5)cos(2\gamma h) + (c_2 + c_4)cos(\gamma h) + c_3,$$

$$A_2 = (c_6 + c_{10})cos(2\gamma h) + (c_7 + c_9)cos(\gamma h) + c_8,$$

$$B = \frac{5\beta\Delta t}{h}sin(2\gamma h) + \frac{50\beta\Delta t}{h}sin(\gamma h),$$

where

$$(c_1 + c_5) = 2 - \frac{40}{h^2} - \frac{20\alpha\Delta t}{h^2}, \quad (c_2 + c_4) = 52 - \frac{80}{h^2} - \frac{40\alpha\Delta t}{h^2}$$

$$(c_6 + c_{10}) = 2 - \frac{40}{h^2} + \frac{20\alpha\Delta t}{h^2}, \quad (c_7 + c_9) = 52 - \frac{80}{h^2} + \frac{40\alpha\Delta t}{h^2}$$

$$c_3 = 66 + \frac{120}{h^2} + \frac{60\alpha\Delta t}{h^2}, \quad c_8 = 66 + \frac{120}{h^2} - \frac{60\alpha\Delta t}{h^2}.$$

From Eq. (4.1), it can be clearly written that

$$|\sigma_1|^2 = \sigma_1\bar{\sigma_1} = \frac{A_1^2 + B^2}{A_2^2 + B^2}$$

and we can say that $A_1 \le A_2$, hence $|\sigma_1| \le 1$. This confirms that numerical scheme (3.9) is unconditionally stable. Secondly, to implement the von Neumann method to Eq. (3.10), first of all, when the U in the nonlinear term UU_x in system (16) is linearized, z_m be going to behave as a local constant, that is, z_m in system (3.10) will be a fixed number. Thus the von Neumann method will become applicable to research the stability of numerical scheme (3.10). Writing the expressions $d_1, d_2, ..., d_9, d_{10}$ that we find in section 3 and $\delta_m^n = e^{i\gamma mh}\zeta^n$ in scheme (3.10), we obtain equations in the following form

$$\sigma_2 = \sigma_B\Big(\frac{\zeta^{n+1}}{\zeta^n}\Big) = \frac{A_3 + iD}{A_4 - iD} \tag{4.2}$$

$$A_3 = (d_1 + d_5)cos(2\gamma h) + (d_2 + d_4)cos(\gamma h) + d_3,$$

$$A_4 = (d_6 + d_{10})cos(2\gamma h) + (d_7 + d_9)cos(\gamma h) + d_8,$$

$$D = \frac{5z_m\Delta t}{h}sin(2\gamma h) + \frac{50z_m\Delta t}{h}sin(\gamma h),$$

where

$$(d_6 + d_{10}) = (d_1 + d_5) = 2 - \frac{40}{h^2},$$

$$(d_7 + d_9) = (d_2 + d_4) = 52 - \frac{80}{h^2},$$

$$d_3 = d_8 = 66 + \frac{120}{h^2}.$$

Here it is clear that $A_3 = A_4$. Hence, $|\sigma_2| \leq 1$ and as a result, we can state that the scheme (3.10) is unconditionally stable since the condition $|\sigma_2| \leq 1$ from Eq. (4.2) is satisfied. In that case, it can be clearly seen that

$$|\rho(\zeta)| \leq |\sigma_1||\sigma_2||\sigma_1|$$

and consequently schemes (3.9) and (3.10) obtained by Strang time-splitting technique are unconditionaly stability.

5. Numerical examples and results

In the present section, we will handle four model problems to visually present the performence and effectiveness of the proposed method. The numerical solution of Equations (3.9) and (3.10) obtained by the second-order Strang splitting algorithms bring about the $(N+1)$ x $(N+1)$ matrix system that are easily and effectively calculated by means of Thomas algorithm. All computer calculations in the study have been carried out with the software Mathlab 2019b on a computer which has a memory 20GB and 64 bit. In order to determine how good the obtained results are, the error norms L_2 and L_∞ characterized in the following are computed

$$L_2 = ||U - U_N||_2 = \sqrt{h\sum_{j=0}^{N}(U - U_N)^2}$$

$$L_\infty = ||U - U_N||_\infty = \max_j |U - U_N|.$$

The BBMB equation given with appropriate initial and boundary conditions has the following three conservation constants

$$
\begin{aligned}
I_1 &= \int_{x_L}^{x_R} U(x,t)dx, \\
I_2 &= \int_{x_L}^{x_R} [U^2(x,t) + U_x^2(x,t)]dx, \\
I_2 &= \int_{x_L}^{x_R} [U^3(x,t) + 3U_x^2(x,t)]dx,
\end{aligned} \tag{5.1}
$$

standing for mass, energy, momentum, respectively. These proportions can be watched in order to control the protected features of the numerical algorithm.

Example 5.1 For the first example, we are going to consider the present equation having the initial condition $U(x,0) = exp(-x^2)$ taking $\alpha = \beta = 1$ in Eq. (1.2) on the domain $[-10, 10]$. Figures 1 and 2 display graphically the numerical approach of Example 5.1 for $\Delta t = 0.01$, $N = 100$ at times $t \leq 10$ and these graphs exhibit the same physical behaviour as in those of [41], [1].

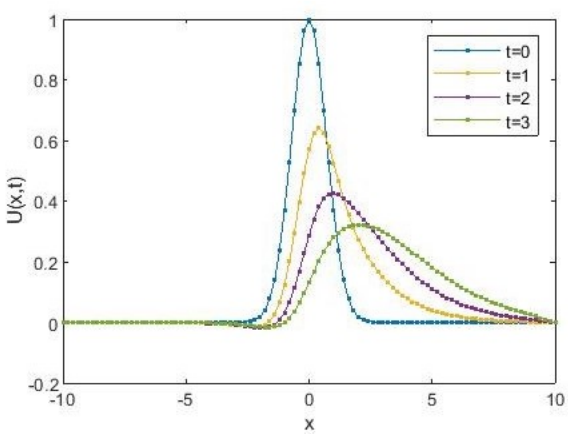

Figure 1. Approximate solutions of Example 5.1 at times $t \in [0, 3]$ for parameters $\alpha = \beta = 1$.

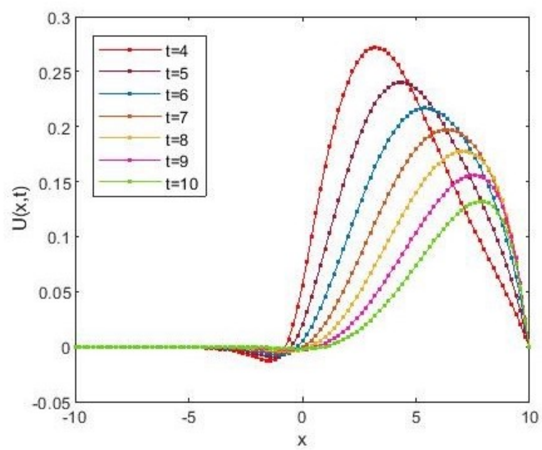

Figure 2. Approximate solutions of Example 5.1 at times $t \in [4, 10]$ for parameters $\alpha = \beta = 1$.

Example 5.2 For the second test problem, we are going to consider the nonhomogeneous BBM-Burgers equation in form

$$
U_t - U_{xxt} - \alpha U_{xx} + \beta U_x + UU_x = F, \qquad x \in [0, \pi], t \in [0, T] \tag{5.2}
$$

in which $F(x,t) = exp(-t)[cosx - sinx + \frac{1}{2}e^{-t}sin(2x)]$. The analytical solution of Eq. (5.2) is presented with $U(x,t) = e^{-t}sinx$ as in [57] and here IC and BCs can be gotten from the analytical solution. All numerical calculations are done for $\Delta t = 0.01$ and $\alpha = \beta = 1$ over the range $[0, \pi]$. Table 1 gives a comparison of the computed L_2 error norm for different values of N at $t = 10$ as in those of [41], [1] and [57]. Table 2 shows a comparison of the error norms L_2 and L_∞ for $N = 121$ and at various time-levels as given in those of [1] and [2]. It can be clearly said from Tables 1 and 2 that the approximate results obtained by the second-order

Strang scheme are quite small. That is, our results are the lowest of all of ones we compare in tables and hence much closer to the exact solutions. Figure 3 shows graphically the numerical approach of Example 5.2 at times $t \leq 8$ and this graph exhibits the same physical behaviour as in [1] and [2].

Table 1. A comparison of the error norm results L_2 of Example 5.2 for various values of N.

N	[41]	[1]	[57]	Present
10	$0.0218e-0$	$1.7147e-4$	$2.9703e-4$	$3.5538e-5$
20	$0.0053e-0$	$5.6341e-5$	$1.1446e-4$	$9.1027e-6$
40	$0.0013e-0$	$-$	$4.9603e-5$	$2.2965e-6$
80	$3.3291e-4$	$7.2635e-6$	$2.3227e-5$	$5.7782e-7$
160	$8.3133e-5$	$-$	$1.1275e-5$	$1.4685e-7$
320	$2.0766e-5$	$8.1631e-7$	$5.5619e-6$	$3.9234e-8$
640	$5.1898e-6$	$-$	$2.7632e-6$	$1.3053e-8$

Table 2. A comparison of the error norm results L_2 and L_∞ of Example 5.2 at various time-levels.

	[1]		[2]		Present	
t	L_2	L_∞	L_2	L_∞	L_2	L_∞
1	$5.13E-03$	$7.67E-03$	$1.51E-03$	$1.46E-03$	$3.01e-05$	$1.34e-04$
2	$1.73E-03$	$2.84E-03$	$1.21E-03$	$1.18E-03$	$1.59e-05$	$5.47e-05$
4	$2.12E-04$	$3.84E-04$	$3.95E-04$	$3.96E-04$	$6.62e-06$	$8.90e-06$
10	$4.08E-06$	$4.06E-06$	$2.75E-06$	$3.22E-06$	$2.54e-07$	$2.21e-07$

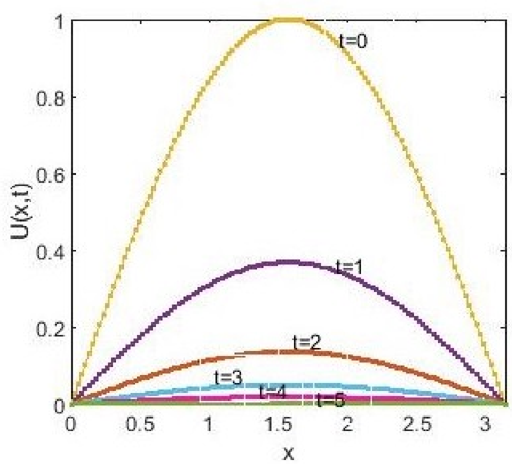

Figure 3. Approximate solutions of Example 5.2 at times $t \leq 5$ for parameters $\alpha = \beta = 1$.

Example 5.3 For the third example, we are going to consider to the numerical approach of Eq. (1.2) presented with the initial condition $U = (x, 0) = sech^2[\frac{x}{4}]$ for $\alpha = 0, \beta = 1$. The analytical solution of this problem is given as in [57]

$$U(x,t) = sech^2[\frac{x}{4} - \frac{t}{3}].$$

Here, we perform a comparison of the solutions of the presented method with the earlier studies in literature for various position and time steps up to $t = 40$ over the region $[-40, 100]$. For this, the error norm values L_2 and L_∞ with invariants I_1, I_2 and I_3 are computed. The computed values are displayed in Tables 3 and 4. This tables clearly exhibit that the results achieved by our scheme are much smaller than those of the others and invariants I_1, I_2 and I_3 are almost the same at increasing time values. This situation shows consistency between the obtained invariants and their exact values. Figure 4 displays the numerical solutions obtained with Strang time-splitting technique at times $t = 0, 10, 20, 30$ and 40 for using parameters $h = 0.05$, $\Delta t = 0.025$. From this figure, it is clear that the single solitary waves go toward right having a constant velocity and protects its amplitude and shape as time progresses. At the beginning, we can say that the single solitary wave whose amplitude is 1 at time $t = 0$, position $x = 0$ and has the same amplitude at time $t = 40$, position $x = 53.35$. Also, the error distribution graph is shown in Figure 5 for the parameter $h = 0.05$, $\Delta t = 0.025$ at time $t = 40$.

Table 3. A comparison of the error norms L_2 and L_∞ at various times on the range $[40, 100]$ of Example 5.3.

		t = 10	t = 20	t = 30	t = 40
$h = 0.2, \Delta t = 0.4$					
Present	L_2	0.00041695	0.00073104	0.000994851	0.01238753
	L_∞	0.00019018	0.00030898	0.00040563	0.00049613
[40]	L_∞	–	–	–	0.10976282
[31]	L_2	0.03195399	0.05446985	0.07306022	0.09025102
	L_∞	0.01477190	0.02321340	0.03003074	0.03638003
$h = \Delta t = 0.1$					
Present	L_2	0.00026149	0.00045867	0.00062439	0.00077763
	L_∞	0.00011930	0.00019395	0.00025496	0.00031177
[40]	L_∞	–	–	–	0.00747237
[31]	L_2	0.00204484	0.00341396	0.00457929	0.00571248
	L_∞	0.00095720	0.00147163	0.00189531	0.00231941
$h = 0.05$, $\Delta t = 0.025$					
Present	L_2	0.00001635	0.00002867	0.00003904	0.00004862
	L_∞	0.00000746	0.00001213	0.00001594	0.00001949
[40]	L_∞	–	–	–	0.00046983
[31]	L_2	0.00012459	0.00025628	0.00040853	0.00055868
	L_∞	0.00005984	0.00010502	0.00016268	0.00021891
$h = 0.2$, $\Delta t = 0.01$					
Present	L_2	0.00000304	0.00000513	0.00000689	0.00000851
	L_∞	0.00000145	0.00000223	0.00000288	0.00000349
[1]	L_2	–	0.00060007	–	–
	L_∞	–	0.00031641	–	–
[31]	L_2	0.00051267	0.00077372	0.00107317	0.00141405
	L_∞	0.00017784	0.00031687	0.00045923	0.00060343

Example 5.4 For the fourth example, we are going to consider for the approximate solution of Equation (1.2) with $\alpha = 0, \beta = 1$. The analytical solution for the test problem can be given as in [57]

$$U = (x, t) = 3c sech^2[k(x - x_0 - vt)]$$

in which $v = 1 + c$ stand for the wave speed and $k = \frac{1}{2}\sqrt{\frac{c}{1+c}}$. This solution represent the movement of a single

Table 4. A comparison of the invariants I_1, I_2 and I_3 at various times on the range $[40, 100]$ of Example 5.3.

		t = 10	t = 20	t = 30	t = 40
$h = 0.2, \Delta t = 0.4$					
Present	I_1	7.99999991	7.99999981	7.99999972	7.99999963
	I_2	5.59999982	5.59999965	5.59999947	5.59999930
	I_3	20.2666611	20.2666560	20.2666530	20.2666512
[31]	I_1	8.0000005	8.0000001	7.9999998	7.9999995
	I_2	5.6000315	5.6000536	5.6000631	5.6000671
	I_3	20.2664360	20.2662535	20.2661684	20.2661288
$h = \Delta t = 0.1$					
Present	I_1	8.00000006	8.00000013	8.00000018	8.00000024
	I_2	5.60000000	5.60000000	5.60000000	5.60000000
	I_3	20.2666667	20.2666666	20.2666666	20.2666666
[31]	I_1	8.0000020	8.0000020	8.0000020	8.0000020
	I_2	5.6000016	5.6000019	5.6000021	5.6000022
	I_3	20.2666713	20.2666716	20.2666717	20.2666718
$h = 0.05, \Delta t = 0.025$					
Present	I_1	8.00000007	8.00000014	8.00000020	8.00000026
	I_2	5.60000000	5.60000000	5.60000000	5.60000000
	I_3	20.2666667	20.2666667	20.2666666	20.2666667
[31]	I_1	7.9999964	7.9999964	7.9999964	7.9999964
	I_2	5.6000010	5.6000010	5.6000010	5.6000010
	I_3	20.2666706	20.2666706	20.2666706	20.2666706
$h = 0.2, \Delta t = 0.01$					
Present	I_1	8.00000006	8.00000011	8.00000017	8.00000022
	I_2	5.60000000	5.60000000	5.60000000	5.60000000
	I_3	20.2666667	20.2666667	20.2666667	20.2666667
[31]	I_1	8.0000009	8.0000009	8.0000009	8.0000009
	I_2	5.6000005	5.6000010	5.6000011	5.6000012
	I_3	20.2666697	20.2666713	20.2666719	20.2666721

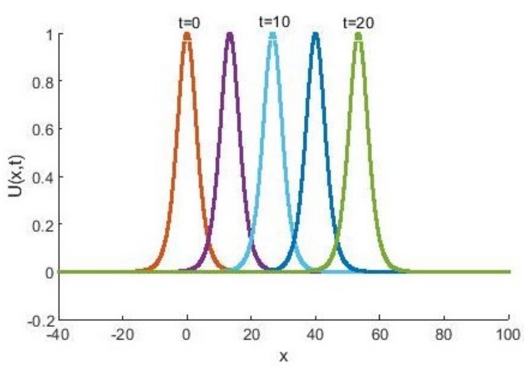

Figure 4. Approximate solutions of Example 5.3 at various times for $h = 0.05, \Delta t = 0.025$ on the solution domain $[-40, 100]$.

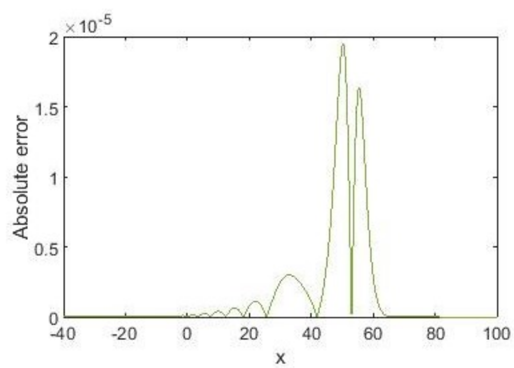

Figure 5. The error distribution graph of Example 5.3 at various times for $\Delta t = 0.025, h = 0.05$ over the region $[-40, 100]$.

solitary wave with amplitude 3c with width k and initially centered at x_0. To be able do a comparison with the earlier studies in literature, the error norm values L_2 and L_∞ with invariants I_1, I_2 and I_3 are computed with the parameters $h = \Delta t = 0.1$ for $c = 0.1$ at the different times over the region $[-40, 60]$. The exact values for the conservative constants are $I1 = 3.9799497$, $I2 = 0.81046249$ and $I3 = 2.579007$ for $c = 0.1$. These calculated values are indicated in Tables 5 and 6. This tables clearly exhibit that the results achieved by our scheme are much smaller than those of the others and invariants I_1, I_2 and I_3 are almost the same at increasing time values. This situation shows consistency between the obtained invariants and their exact values. Figure 6 displays the numerical solutions obtained with Strang time-splitting technique at various times $t = 0, 5, 10, 15$ and 20. From this figure, it is clear that the single solitary waves go to right with a fixed velocity and protects its amplitude and shape as time progresses. At the beginning, we can say that the single solitary wave whose amplitude is 0.3 at time $t = 0$, position $x = 0$ and has the same amplitude at time $t = 20$, position $x = 22$. Also, the error distribution graph is shown in Figure 7 at time $t = 20$.

Table 5. A comparison of error norms L_2 and L_∞ for $\Delta t = h = 0.1$, $c = 0.1$ at various times on the range $[-40, 60]$ for Example 5.4.

Method	Error	t				
		4	8	12	16	20
Present	$L_2 x10^3$	0.00829132	0.01652186	0.02400207	0.03060004	0.03710617
	$L_\infty x10^3$	0.00436056	0.00556405	0.00662545	0.00875511	0.01268449
[22]	$L_2 x10^3$	39.82	79.46	118.8	157.7	196.1
	$L_\infty x10^3$	13.74	27.66	41.35	54.60	67.35
[15]	$L_2 x10^3$	0.0006	0.0026	0.0064	0.0115	0.0184
	$L_\infty x10^3$	0.1458	0.5786	0.9223	1.2148	1.5664
[16]	$L_2 x10^3$	0.116	0.224	0.325	0.417	0.511
	$L_\infty x10^3$	0.054	0.100	0.139	0.171	0.198
[17]	$L_2 x10^3$	–	–	–	–	0.30
	$L_\infty x10^3$	–	–	–	–	0.116
[32]	$L_2 x10^3$	0.12	0.23	0.34	0.45	0.55
	$L_\infty x10^3$	0.05	0.09	0.14	0.18	0.21
[20]	$L_2 x10^3$	0.048	0.094	0.138	0.180	0.219
	$L_\infty x10^3$	0.019	0.038	0.056	0.071	0.086
[1]	$L_2 x10^3$	0.042	0.033	0.13	0.16	0.20
	$L_\infty x10^3$	0.015	0.033	0.049	0.064	0.078
[55]	$L_2 x10^3$	0.0149	0.0271	0.0364	0.0429	0.0476
	$L_\infty x10^3$	0.0060	0.0105	0.0132	0.0145	0.0150
[56]	$L_2 x10^3$	0.0646	0.1282	0.1901	0.2498	0.3072
	$L_\infty x10^3$	0.0250	0.0505	0.0747	0.0971	0.1177
[53]	$L_2 x10^3$	0.0169	0.0329	0.0474	0.06039	0.0723
	$L_\infty x10^3$	0.0072	0.0141	0.0199	0.0247	0.0288
[31]	$L_2 x10^3$	0.0475	0.0929	0.1365	0.1773	0.2162
	$L_\infty x10^3$	0.0188	0.0379	0.0553	0.0706	0.0846
[57]	$L_2 x10^3$	0.0203	0.0383	0.0525	0.0630	0.0719
	$L_\infty x10^3$	0.0084	0.0160	0.0210	0.0241	0.0270

6. Conclusion

In this work, the approximate solution of the BBM-Burgers equation with convenient initial and boundary conditions is obtained using Strang time-splitting technique via finite element collocation method (FEM) with quintic B- spline. The efficiency and accuracy of the present method are demonstrated on four examples. The

Table 6. A comparison of I_1, I_2 and I_3 invariants for $c = 0.1$, $\Delta t = h = 0.1$ at various times on the range $[40, 60]$ for Example 5.4.

		t = 0	t = 4	t = 8	t = 12	t = 16	t = 20
Present	I_1	3.97992702	3.97995533	3.97997867	3.97999973	3.98001245	3.97999912
	I_2	0.81046249	0.81046249	0.81046249	0.81046249	0.81046249	0.81046249
	I_3	2.57900744	2.57900744	2.57900744	2.57900744	2.57900744	2.57900744
[22]	I_1	–	4.42017	4.41822	4.41623	4.41423	4.41219
	I_2	–	0.899873	0.899236	0.898601	0.897967	0.897342
	I_3	–	2.86339	2.86106	2.85863	2.85613	2.85361
[16]	I_1	3.97993	3.98039	3.98083	3.98125	3.98165	3.98206
	I_2	0.810461	0.810610	0.810752	0.810884	0.811014	0.811164
	I_3	2.57901	2.57950	2.57996	2.58041	2.58083	2.58133
[32]	I_1	3.97992	3.97995	3.97997	3.97999	3.97999	3.97997
	I_2	0.810459	0.810459	0.810459	0.810459	0.810459	0.810459
	I_3	2.57901	2.57901	2.57901	2.57901	2.57901	2.57901
[20]	I_1	3.97993	3.97993	3.97993	3.97992	3.97991	3.97988
	I_2	0.810465	0.810465	0.810465	0.810465	0.810465	0.810465
	I_3	2.57901	2.57901	2.57901	2.57901	2.57901	2.57901
[55]	I_1	–	3.97993	3.97993	3.97993	3.97992	3.97988
	I_2	–	0.810462	0.810462	0.810463	0.810463	0.810464
	I_3	–	2.57901	2.57901	2.57901	2.57901	2.57901
[56]	I_1	–	3.97993	3.97993	33.9799	3.97992	3.97988
	I_2	–	0.810461	0.810461	0.810461	0.810461	0.810461
	I_3	–	2.579	2.579	2.579	2.579	2.579
[53]	I_1	3.979927	3.979954	3.979971	3.979984	3.979987	3.979962
	I_2	0.810462	0.810462	0.810462	0.810462	0.810462	0.810462
	I_3	2.579007	2.579007	2.579007	2.579007	2.579007	2.579007
[31]	I_1	3.9799274	3.9799294	3.9799277	3.9799250	3.9799164	3.9798820
	I_2	0.8104627	0.8104627	0.8104627	0.8104627	0.8104627	0.8104627
	I_3	2.5790082	2.5790082	2.5790083	2.5790083	2.5790083	2.5790083

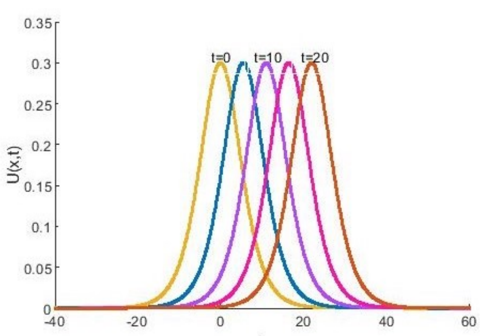

Figure 6. Approximate solutions of Example 5.4 for $h = \Delta t = c = 0.1$ over the region $[-40, 60]$.

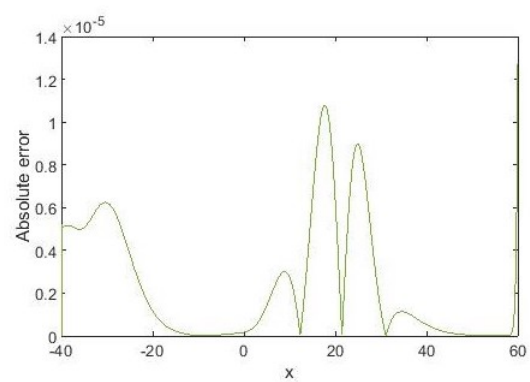

Figure 7. The error distribution graph of Example 5.4 for $h = \Delta t = c = 0.1$ over region $[-40, 60]$.

error norms L_2 and L_∞ with invariants I_1, I_2 and I_3 are calculated and compared by other studies in the literature. The new results achieved from the numerical approach show that the error norms L_2 and L_∞ are fairly small and invariants I_1, I_2 and I_3 reasonably protect and remain almost constant during computer run time. The results produced in the article have been compared with some existing studies in the literature in the form of tables and graphics, and it can be said that the approach used in our study produces very good results. As a result, we can easily say that this technique is easy to apply and useful in obtaining more accurate numerical results.

References

[1] Arora G, Mittal RC, Singh BK. Numerical solution of BBM-Burger equation with quartic B-Spline collocation Method. Journal of Engineering Science and Technology Special issue on ICMTEA 2013 Conference 2014; 104-116.

[2] Arora S, Jain R, Kukreja VK. Solution of Benjamin-Bona-Mahony-Burgers equation using collocation method with quintic Hermite splines. Applied Numerical Mathematics 2020; 154: 1-16.

[3] Al-Khaled K, Momani S, Alawneh A. Approximate wave solutions for generalized Benjamin–Bona–Mahony–Burgers equations. Applied Mathematics and Computation 2005; 171: 281-292.

[4] Alquran M, Al-Khaled K. Sinc and solitary wave solutions to the generalized Benjamin– Bona–Mahony–Burgers equation. Physica Scripta 2011; 83: 065010,6 pages.

[5] Benjamin T.B, Bona JL, Mahony J.J. Model equations for waves in nonlinear dispersive systems. Philosophical Transactions of the Royal Society,London 1972; 227: 47-78.

[6] Bhardwaj D, Shankar RA. Computational method for regularized long wave equation. Computers and Mathematics with Applications 2000; 40: 1397-1404.

[7] Bruzon M.S, Gandarias ML. Travelling wave solutions for a generalized Benjamin- Bona-Mahony-Burgers equation. International Journal of Mathematical Models and Methods in Applied Sciences 2008; 2: 103-108.

[8] Blanes S, Casas F. A concise introduction to geometric numerical integration Boca Raton: CRC Press, 2016.

[9] Başhan A, Yağmurlu NM. A mixed method approach to the solitary wave, undular bore and boundary-forced solutions of the Regularized Long Wave equation. Computational and Applied Mathematics 2022; 41 (169): https://doi.org/10.1007/s40314-022-01882-7

[10] Başhan A. A novel outlook to the an alternative equation for modelling shallow water wave: Regularised Long Wave (RLW) equation. Indian Journal of Pure and Applied Mathematics 2022; https://doi.org/10.1007/s13226-022-00239-4

[11] Başhan A. Single Solitary Wave and Wave Generation Solutions of the Regularised Long Wave (RLW) Equation. Gazi University Journal of Science 2022; 35 (4): 1597-1612.

[12] Başhan A, Yağmurlu NM, Uçar Y, Esen A. A new perspective for the numerical solution of the Modified Equal Width wave equation. Mathematical Methods in the Applied Science 2021; 44: 8925-8939.

[13] Başhan A, Yağmurlu NM, Uçar Y, Esen A. Finite difference method combined with differential quadrature method for numerical computation of the modified equal width wave equation. Numerical Methods for Partial Differential Equation.2021; 37: 690–706.

[14] Bulut F, Oruç Ö, Esen A. Higher order Haar wavelet method integrated with strang splitting for solving regularized long wave equation. Mathematics and Computers in Simulation 2022; 197: 277-290.

[15] Dağ İ, Özer MN. Approximation of RLW equation by least square cubic B-spline finite element method. Applied Mathematical Modelling 2001; 25: 221-231.

[16] Dogan,A. Numerical solution of RLW equation using linear finite elements within Galerkin's method. Applied Mathematical Modelling 2002; 26: 771-783.

[17] Dağ İ, Saka B, Irk D. Application of cubic B-splines for numerical solution of the RLW equation. Applied Mathematics and Computation 2004; 159: 373-389.

[18] Dehghan M, Shafieeabyaneh N, Abbaszadeh M. Numerical and theoretical discussions for solving nonlinear generalized Benjamin–Bona–Mahony–Burgers equation based on the Legendre spectral element method. Numerical Methods for Partial Differential Equation 2021; 7 (1): 360-382.

[19] Dag I. Studies of B-spline finite elements. Ph.D. Thesis, University College of North Wales, Bangor, Gwynedd, 1994.

[20] Esen A, Kutluay S. Application of a lumped Galerkin method to the regularized long wave equation. Applied Mathematics and Computation 2006; 174: 833-845

[21] Fakhari A, Domairry G, Ebrahimpour. Approximate explicit solutions of nonlinear BBMB equations by homotopy analysis method and comparison with the exact solution. Physics Letters A 2007; 368: 64-68.

[22] Gardner LRT, Gardner GA, Dağ İ. A B-spline finite element method for the regularized long wave equation. Communications in Numerical Methods in Engineering 1995; 11: 59-68.

[23] Gardner LRT, Gardner GA, Dogan A. A least-squares finite element scheme for the RLW equation. Communications in Numerical Methods in Engineering 1996; 12: 795-804.

[24] Gustafsson B. High order difference methods for time dependent PDE. In Springer series in computational mathematics, Springer-Verlag, Berlin, New York, Heidelberg 2007; vol. 38.

[25] Geiser J, Bartecki K. Additive multiplicative and iterative splitting methods for Maxwell equations. Algorithms and applications AIP Conference Proceedings 2018; 1978: 470002.

[26] Geiser J. Decomposition methods for differential equations. Theory and applications in Chapman, Hall/CRC numerical analys is and scientific computingseries, Boca Raton: CRC Press, Taylor Francis Group 2009.

[27] Hundsdorfer W, Verwer J. Numerical Solution of Time-Dependent Advection-Diffusion-Reaction Equations (First Edition). Springer-Verla Berlin Heidelberg 2003.

[28] Holden H, Korlsen KH, Lie K-A, Risebro N.H. Splitting methods for partial differential equations with rough solutions. European Mathematical Society, Publishing House, Zürich 2010.

[29] Jain MK. Numerical solution of differential equations. New Delhi: John Wiley Sons, (Asia) private limited 1984.

[30] Jain PC, Shankar R, Singh TV. Numerical solution of regularized long-wave equation. Communications in Numerical Methods in Engineering 1993; 9 (7): 579-586.

[31] Karakoc SBG, Bhowmik SK. Galerkin finite element solution for Benjamin– Bona–Mahony–Burgers equation with cubic B-splines. Computers and Mathematics with Applications 2019; 77: 1917–1932.

[32] Kutluay S, Esen A. A finite difference solution of the regularized long wave equation. Mathematical Problems in Engineering 2006; 1-4. DOI: 10.1155/MPE/2006/85743

[33] Kutluay S, Karta M, Uçar Y. Strang time-splitting technique for the generalised Rosenau–RLW equation. Pramana Journal of Physics 2021; 95:148. https://doi.org/10.1007/s12043-021-02182-1

[34] Kadri T, Khiari N, Abidi F, Omrani K. Methods for the numerical solution of the Benjamin-Bona-Mahony-Burgers equation. Numerical Methods for Partial Differential Equations 2008; 24 (6): 1501–1516.

[35] Karakoç SBG, Geyikli T, Başhan A. A Numerical Solution of the Modified Regularized Long Wave (MRLW) Equation Using Quartic B-Splines. TWMS Journal of Applied and Engineering Mathematics 2013; 3 (2): 231-244.

[36] Kondo C, Webler CM. Higher-order for the generalized BBM-Burgers Equation: Existence and convergence Results. Applicable Analysis An International Journal 2009; 88 (7): 1-17.

[37] Lai S, Lv X, Shuai M. The Jacobi elliptic function solutions to a generalized Benjamin-Bona-Mahony equation. Mathematical and Computer Modelling 2009; 49: 369-378.

[38] Marchuk, GI. Some application of splitting-up methods to the solution of mathematical physics problems. Aplikace matematiky 1968; 13 (2): 103-132.

[39] McLachlan RI, Quispel GRW. Splitting methods. Acta Numerica 2001; 341-434. https://doi.org/10.1017/S0962492902000053

[40] Mohebbi A, Faraz Z. Solitary wave solution of nonlinear Benjamin–Bona–Mahony–Burgers equation using a high-order difference scheme. Computational and Applied Mathematics 2017; 36: 915–927.

[41] Omrani K, Ayadi M. Finite difference discretization of the Benjamin-Bona-Mahony-Burgers equation. Numerical Methods for Partial Differential Equations 2007; 24 (1): 239-248.

[42] Oruç Ö, Esen A, Bulut F. A strang splitting approach combined with Chebyshev wavelets to solve the regularized long-wave equation numerically. Mediterranean Journal of Mathematics 2020; 17 (5): 1-18.

[43] Peregrine DH. Calculations of the development of an undular bore. Journal of Fluid Mechanics 1966; 25 (2): 321-330.

[44] Prenter PM. Splines and variational methods. Wiley, New York 1975.

[45] Raupp MA. Galerkin Methods Applied to the Benjamin-Bona-Mahony Equation. Boletim da Sociedade Brasileira de Matemática 1975; 6: 65-77.

[46] Soliman AA, Raslan KR. Collocation method using quadratic B-spline for the RLW equation. International Journal of Computer Mathematics 2001; 78: 399-412.

[47] Soliman AA, Hussien MH. Collocation solution for RLW equation with septic spline. Applied Mathematics and Computation 2005; 161: 623-636.

[48] Seydaoğlu M, Blanes S. High-order splitting methods for separable non-autonomous parabolic equations. Applied Numerical Mathematics 2014; 84: 22-32.

[49] Smith G. D. Numerical solutions of partial differential equations: Finite difference methods. Clarendon Press,Oxford, 1985.

[50] Strang G. On the construction and comparison of difference schemes. SIAM Journal on Numerical Analysis 1968; 5: 506-517.

[51] Trotter HF. On the product of semi-groups of operators. Proceedings of the American Mathematical Society 1959; 10: 545-551.

[52] Uçar Y, Yağmurlu NM, Çelikkaya İ. Numerical Solution of Burger's Type Equation Using Finite Element Collocation method with Strang Splitting. Mathematical Sciences and Applications E-Notes 2020; 8 (1): 19-45.

[53] Yagmurlu NM, Ucar Y, Celikkaya İ. Operator Splitting For Numerical Solutions Of The RLW Equation. Journal of Applied Analysis and Computation 2018; 8 (5): 1494-1510. http://jaac-online.com/DOI:10.11948/2018

[54] Zarebnia M, Parvaz R. Cubic B-spline collocation method for numerical solution of the Benjamin-Bona-Mahony-Burgers equation. International Journal of Mathematics and Computer Science 2013; 7 (3): 540-543.

[55] Zarebnia M, Parvaz R. On the numerical treatment and analysis of Benjamin –Bona –Mahony –Burgers equation. Applied Mathematics and Computation 2016; 284: 79-88.

[56] Zarebnia M, Parvaz R. Numerical study of the Benjamin-Bona-Mahony-Burgers equation. Boletim da Sociedade Paranaense de Matematica 2017; 35 (1): 127-138.

[57] Zarebnia M, Parvaz R. Error Analysis of the Numerical Solution of the Benjamin- Bona-Mahony-Burgers Equation. Boletim da Sociedade Paranaense de Matematica 2020; 38(3) 177–191. https://doi.org/10.5269/bspm. v38i3.34498

[58] Zhang Q, Liu L, Zhang J. The numerical analysis of two linearized difference schemes for the Benjamin–Bona–Mahony–Burgers equation. Numerical Methods for Partial Differential Equations 2020; 36 (6): 1790-1810.

[59] Zurnacı F, Gücüyenen N, Seydaoğlu M, Tanoğlu G. Convergence analysis and numerical solution of the Benjamin–Bona–Mahony equation by Lie–Trotter splitting. Turkish Journal of Mathematics 2018; 42: 1471-1483.